Electron localization in Co/Ni superlattices

Sihong Kim, D. Lederman, J. M. Gallego, and Ivan K. Schuller

Physics Department 0319, University of California–San Diego, La Jolla, California 92093-0319

The residual resistivity in Co/Ni superlattices is shown to oscillate as a function of superlattice period for fixed Co to Ni thickness ratio. Additional experimental evidence shows that this behavior is enhanced when randomness is artificially introduced in the individual layer thickness. We analyze this in terms of a scattering mechanism associated with the presence of localized electron eigenstates near the Fermi level in the metallic superlattices. A one-dimensional tight-binding calculation shows that localized states appear close to superlattice periods for which the resistivity exhibits maxima. [S0163-1829(96)50632-6]

Since the introduction of the superlattice concept,[1] much progress has been made in engineering new types of materials with interesting physical properties. Recent improvements in the quantitative structural analysis of thin films make the identification of *intrinsic* properties *unrelated* to structural disorder possible.[2] The successful growth and thorough structural characterization of ferromagnetic/ferromagnetic Co/Ni was recently reported.[3] Subsequently, an oscillatory dependence of the resistivity (ρ) and anisotropic magnetoresistance (AMR) on the Co or Ni thickness in Co/Ni superlattices was discovered.[4] Possible explanations of these oscillations are zone folding of the superlattice energy band and electron localization. In this paper, we report on further experiments which indicate that electron localization may be responsible for the oscillations. A model calculation of the energy eigenvalues of the localized states, based on a one-dimensional tight-binding model, is consistent with the observed resistivity oscillations.

Epitaxial Co/Ni (fcc/fcc) superlattices were grown by molecular-beam epitaxy (MBE) along the [111] direction on single crystal [11.0] sapphire substrates. Sample growth, structural characterization, and resistivity measurements were similar to those presented previously.[3,4]

Figure 1(a) shows the 4.2 K resistivity as a function of the superlattice modulation period Λ for a fixed ratio of Co to Ni atomic planes in each bilayer, denoted as $(Co_{0.6\Lambda}/Ni_{0.4\Lambda})_N$. The number of bilayers N in each sample was adjusted to make the total thickness of the film be ~ 1000 Å. Two oscillations of the resistivity are clearly observed. The peak to peak amplitude of the oscillations is about 2 $\mu\Omega$ cm. The overall resistivity is small compared to other typical published resistivities of metallic multilayers. This may be a result of the high structural quality of the samples together with the low intrinsic resistivity of the Co/Ni alloys.[5] In samples with higher resistivities, the oscillations may be difficult to observe due to the large background. Since the relative concentration of Co and Ni is kept constant, this effect cannot be due to significant sample alloying.

The mean free path of these samples is limited by the in-plane grain sizes[4] (~ 200 Å) and the resistivity of a co-evaporated Co/Ni alloy of comparable concentration is ~ 4.6 $\mu\Omega$ cm. This indicates that interface scattering is relatively small and the mean free path along the superlattice direction is longer than Λ. This makes the observation of superlattice effects possible.

Figure 1(b) shows the 300 K resistivity for the same set of samples. Within the experimental uncertainty the oscillation amplitude is identical to the one at 4.2 K. This indicates that it is the residual resistivity which oscillates.

For several samples the resistivity was measured in the 4.2–300 K temperature range. When the residual resistivity was subtracted, the data fell on a universal curve within the experimental error as shown in Fig. 2. In the low-temperature range below 18 K, the resistivity exhibits a T^2 dependence, implying that the dominant mechanism responsible is electron-electron scattering, which is consistent with bulk Co and Ni resistivity measurements.[6] However, the coefficient of T^2 term are $\sim 3 \times 10^{-5}$ $\mu\Omega$ cm/K^2, $2-3$ times larger than reported bulk values for Co or Ni. The changes in the coefficients of T^2 are much smaller than the oscillations observed for the residual resistivities, i.e., the temperature-dependent portion of the resistivity is not affected significantly by the superlattice structure.

In order to examine the effect of randomness on the electron transport, a series of samples were made with random layer thickness variations ("fluctuation") in each bilayer intentionally introduced during the growth process. The same fluctuation pattern was used for all samples, but their width was varied to produce different amounts of disorder. The total number of bilayers was ≥ 25 in order to avoid statistical artifacts. Since all other growth parameters were identical to
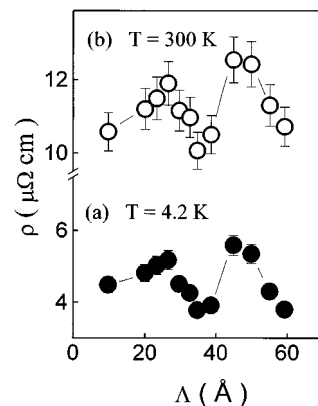

FIG. 1. Average resistivity for a series of $(Co_{0.6\Lambda}/Ni_{0.4\Lambda})_N$ as a function of Λ in Å at two different temperatures, (a) $T = 4.2$ K and (b) $T = 300$ K. The solid lines are guides to the eye.
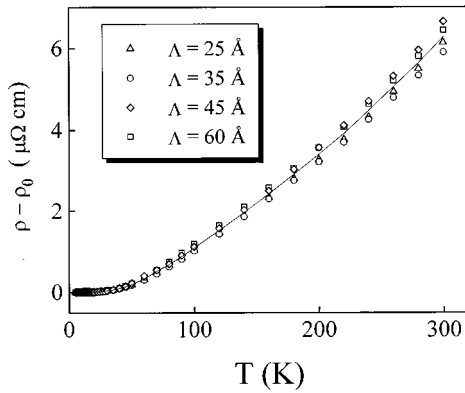
FIG. 2. Average resistivity with residual resistivity subtracted. The solid line is the average of the data shown.

other Co/Ni superlattices, we believe that structural properties such as interface roughness, chemical sharpness of the interface, and other uncontrolled structural defects should be similar for all samples in this series.

Three series of samples were prepared with average superlattice modulation periods $\bar{\Lambda}=25$, 30, and 35 Å . These values were chosen because they represent a local maximum, intermediate, and minimum of the resistivity in Fig. 1. The superlattice structure was analyzed using x-ray diffraction (XRD). As the layer thickness variation increased, the superlattice peaks broadened and decreased in intensity with respect to the main Bragg peak, while the main Bragg peak position remained unchanged as expected. Other x-ray structural parameters, such as the full width at half maximum (FWHM) of θ–2θ peaks, sharpness of the finite size peaks of the low angle spectra, and the width of the rocking curve of the central XRD peak, were similar for all samples.

Figure 3 shows the 4.2 K resistivity as a function of an artificially introduced Gaussian layer thickness fluctuation σ for these three series. In all cases, there is an increase in resistivity with σ. The resistivity increase in the $\bar{\Lambda}=25$ Å samples, which have higher resistivities, is very clear. However, the resistivity in the $\bar{\Lambda}=35$ Å series seems affected very little. The $\bar{\Lambda}=30$ Å series show the intermediate behavior. This indicates that the amplitude of the resistivity oscil-

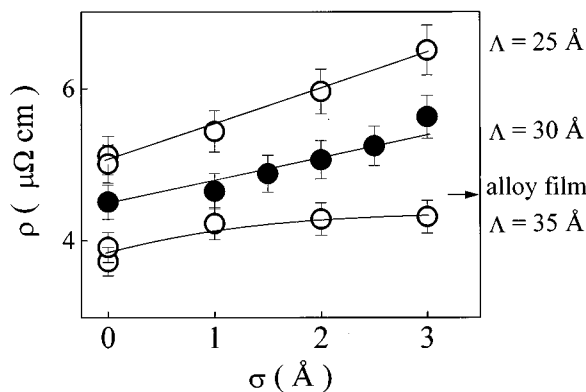lations may be enhanced by slight disorder induced in the periodicity. It is interesting to note that the resistivity of the $\bar{\Lambda}=35$ Å samples saturates somewhat below the alloy resistivity, which could be considered as the upper limit for the interface scattering, while the $\bar{\Lambda}=25$ Å samples have higher resistivities than the alloy, which implies the presence of a different scattering mechanism.

Based on the above experimental results, we evaluated the proposed mechanisms in Ref. 4, *the minigap model*, associated with the zone folding of the superlattice energy band, and *electron localization*.

In the minigap model, the energy band is divided into minibands associated with the reduced size of the superlattice Brillouin zone (BZ). As a consequence, energy minigaps appear at each of the superlattice BZ boundary. The energy minigap changes the density of states (DOS) at the Fermi level or reduces the mobility due to an increase of the effective mass. If the Fermi level lies in the minigap, the resistivity increases.[7] Energy minigaps were recently observed in Ag/Au superlattices grown along the [111] direction using photoemission spectroscopy.[8]

There are three possible reasons why the data perhaps are not consistent with the minigap model. First, because the temperature-dependent resistivity is almost sample independent, the contribution from dynamic scattering mechanisms, such as electron-electron, electron-magnon, or electron-phonon scattering, are similar in all samples. Moreover, if the minigaps are smaller than ~ 50 meV, large variation in the temperature dependence should be observed especially for the samples at the peak in the resistivity. This implies that the DOS at the Fermi level may not be significantly affected. Second, if the resistivity oscillations are caused by energy minigaps at the Fermi level, their amplitude is expected to decrease with increasing disorder as the modulation period becomes more diffuse. The data in Fig. 3 clearly contradict this prediction. Finally, according to the miniband model, the resistivity is primarily dependent on Λ because the energy minigaps appear only at the superlattice BZ boundary. The Co and Ni thickness in each bilayer could have an indirect impact on the resistivity by causing the Fermi level to move and/or the band structure to change. The residual resistivity for the samples which have the same superlattice modulation period, $\Lambda=50$ Å , exhibit two oscillations of comparable amplitude as a function of the Co concentration between 15% and 60%. Together with the data in Ref. 4, it is clear that the residual resistivity is a function of both the Co and Ni thicknesses. However, a realistic band-structure calculation may perhaps reconcile these observations with the minigap model.

Due to these experimental facts, described above, we explore an alternative model which may describe semiquantitatively the data. We assume that most of the conduction come from the extended s bands[9] and that some of the d electrons are localized in the superlattices.[10] Then, we calculated the energy eigenvalues for the localized d electrons at each superlattice period. These d-electron states cross the Fermi level at particular values of the superlattice period. If these localized states, close to the Fermi level, give rise to strong scattering with the conduction s electrons, they may give rise to an increase in the resistivity.

FIG. 3. Average resistivity for $(Co_{0.6\Lambda}/Ni_{0.4\Lambda})_N$, $\Lambda=25$, 30, and 35 Å as a function of layer thickness variation, σ. The arrow indicates Co/Ni alloy resistivity. The solid lines are guides to the eye.

The chemical composition of a superlattice along the growth direction can be represented by a one-dimensional sequence of binary numbers. For example, a Co/Ni superlattice with $\Lambda = 5a$ (a, a lattice spacing) and Co to Ni ratio = 3/2 can be described as a sequence of occupations $\{\Omega_n\} = \{\cdots 1\,1\,1\,0\,0\,1\,1\,1\,0\,0\cdots\}$, which is perfectly periodic. However, this sequence is altered if Λ/a is an irrational number and/or disorder with a finite interface width σ_{in} is present. This disorder can be introduced into a model in two ways: (i) assuming that Ω_n is randomly distributed or (ii) by taking a quasiperiodic sequence for[11] Ω_n. A superlattice potential can be generated by each sequence $\{\Omega_n\}$:

$$V(x) = \sum_n \Omega_n V_{\text{Co}}(x - na) + (1 - \Omega_n) V_{\text{Ni}}(x - na), \quad (1)$$

where Ω_n represents the occupation of Co atoms at site n.

For the model calculation described below, we assume a quasiperiodic sequence for Ω_n. In this case, the potential can be decomposed into two parts: V_P, which is periodic, and V_A, which is aperiodic with respect to a. To perform a calculation, we decomposed the potential in accordance with the scheme introduced by Ref. 12:

$$V_P(x) = \sum_n V_+(x - na), \quad V_A(x) = \sum_n \tau_n V_-(x - na),$$
$$(2)$$

with

$$V_\pm(x) = 1/2[V_{\text{Co}}(x) \pm V_{\text{Ni}}(x)], \quad \tau_n = (2\Omega_n - 1). \quad (3)$$

We investigated a d-electronic state in the Hamiltonian $H = T + V_P + V_A$, where T is the kinetic energy operator, using the tight-binding approximation. The eigenfunction with eigenvalue E can be written as

$$|\Psi\rangle = \sum_n f_n |n\rangle, \quad (4)$$

where $|n\rangle$ denotes a Wannier state localized around site n and f_n satisfies the following recurrence relation:

$$V_H(f_{n-1} + f_{n+1}) = (E - \tau_n \varepsilon_- - \varepsilon_+) f_n, \quad (5)$$

where

$$\varepsilon_+ = \langle n | T + V_+(x - na) | n \rangle, \quad \varepsilon_- = \langle n | V_-(x - na) | n \rangle,$$

$$V_N = \langle n | T + V_+(x - na) | n+1 \rangle. \quad (6)$$

All other terms are discarded as higher-order corrections because both $V_\pm(x - an)$ and $|n\rangle$ are localized around the nth site.

If $\varepsilon_- = 0$, Eq. (5) represents a one-dimensional energy band of width $4V_H$ centered around ε_+. Therefore, parameters can be estimated from band-structure calculations of fcc Co and fcc Ni.[13] The $3d$ bands of Co and Ni have about the same width ~ 5 eV ($= 4V_H$). ε_- is estimated from the relative position of the minority spin bands of Co and Ni, which are responsible for electronic transport. The Co band is shifted by ~ 1 eV ($= 2\varepsilon_-$) with respect to the Ni band. The
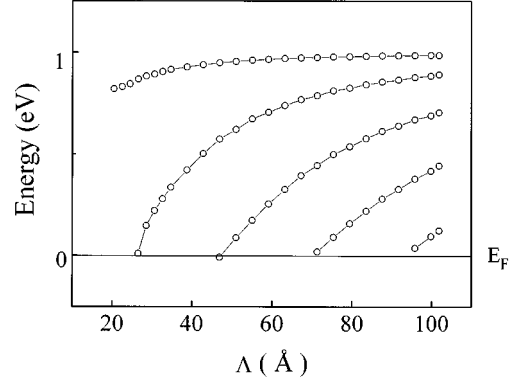

FIG. 4. Energy eigenvalues for $(\text{Co}_{0.6\Lambda}/\text{Ni}_{0.4\Lambda})_N$ measured from the bulk Fermi level as described in the text. The superlattice Fermi level is drawn at the bulk Fermi level. The solid lines are guides to the eye.

energy level is referenced to the bulk Fermi level, which is ~ 1 eV below the Co band edge and close to the Ni band edge.

We calculated the energy eigenvalues of the localized states for each superlattice, represented by a sequence $\{\tau_n\}$ with interface range $2\sigma_i = 2$ ML. We used the method developed by Luban $et\ al.$,[12] which finds the doubly minimal solution (DMS) of Eq. (5) numerically using the backward iteration technique, which is free of numerical instabilities inherent in second-order difference equations.

We compared the energy eigenvalues, using two different methods of generating the sequence $\{\tau_n\}$. One is to use a truly quasiperiodic sequence $\{\tau_n\}$, which assumes a continuous change between 1 and -1 only at the interfaces. The other is to use $\{\tau_n\}$, entirely composed of binary numbers but with a weighted random distribution of 1's and -1's at the interfaces. The energy eigenvalues are obtained by averaging over different ensembles. We found no significant differences in the calculated energy eigenvalues between the two methods. The reason for this is that the eigenvalues are mainly determined by the values of τ_n away from the interface, which is a small fraction of the entire superlattice for large Λ's.

In solving Eq. (7), several $localized$ states appear near the band edge, which show strong spatially nonuniform site probability, $|f_n|^2$. These states could provide an additional scattering mechanism for the $4s$ electrons, which are the dominant charge carriers in Co or Ni. We should point out that not all the energy eigenstates are localized in this model.

Figure 4 shows the energy eigenvalues of the $localized$ states, found at each superlattice period Λ for the samples shown in Fig. 1. The extended state bands appearing further from the band edge are not shown in Fig. 4. The superlattice Fermi level in Fig. 4 is drawn at the bulk Fermi level, which is used as a reference energy. This is somewhat arbitrary because the Fermi level of a superlattice may be higher than the bulk and may also depend on Λ.[14]

The localized states near the Fermi level appear at $\Lambda = \sim 26$ and ~ 48 Å. The systematic reappearance of localized states near the Fermi level may explain the oscillatory behavior in the residual resistivity. Although we cannot quantitatively predict the magnitude of the oscillations, the agreement with the data in Fig. 1, which shows resistivity

maxima at $\Lambda = \sim 25$ and ~ 50 Å , is remarkable. A close analogy can be found in dilute alloy systems,[15] especially transition-metal impurities in Cu.[16] For 1 at. % Cr impurities in Cu the residual resistivity increases by ~ 20 $\mu\Omega$ cm when the *virtual bound state* at the Cr site lies near the Fermi level. When Cr is substituted by Ni, the increase is only ~ 1 $\mu\Omega$ cm because for Ni the virtual bound state lies well below the Fermi level.

We expect that effective scattering cross section would be smaller and decrease faster in energy in the present case because the localization occurs only along the growth direction. More sophisticated models, which include multiple bands and three-dimensional crystal structure, are necessary to understand this phenomenon quantitatively. The fraction of d electrons which are localized and the size of the scattering cross section are still open issues.

Although the nature of d electrons in transition metals, itinerant or localized, is controversial, we have shown here that their properties could be affected by the superlattice structure. As for the s electrons, it is hard to imagine that almost free s electrons can be localized by a small perturbation due to superlattice structure.

In summary, the resistivity of Co/Ni superlattices oscillates as function of Co, Ni, and superlattice modulation period. The oscillations increase in amplitude as the disorder of the modulation period is increased. A one-dimensional tight-binding model calculation implies the existence of localized d states with energies close to the Fermi surface at periodicities where the resistivity is enhanced. These localized states possibly provide the additional scattering needed for the presence of resistivity oscillations.

[1] L. Esaki and R. Tsu, IBM J. Res. Dev. **14**, 61 (1970).

[2] For a review, see Quantitative Analysis of Thin Films pts. I&II in special issues of, respectively, Mater. Res. Soc. Bull. **XVII** (12), XXX (1992) and **XVIII** (1), XXX (1993). Edited by Y. Bruynseraede and Ivan K. Schuller.

[3] J. M. Gallego, S. Kim, T. J. Moran, D. Lederman, and Ivan K. Schuller, Phys. Rev. B **51**, 2550 (1995).

[4] J. M. Gallego, D. Lederman, S. Kim, and Ivan K. Schuller, Phys. Rev. Lett. **74**, 4515 (1995).

[5] S. U. Jen, T. P. Chen, and S. A. Chang, J. Appl. Phys. **70**, 5831 (1991).

[6] P. Radhakrishna and M. Nielsen, Phys. Status Solidi **11**, 111 (1965); G. K. White and S. B. Woods, Philos. Trans. R. Soc. London Ser. A **251**, 273 (1959).

[7] J. C. Slater, Phys. Rev. **84**, 179 (1951); J. Koehler, Phys. Rev. B **23**, 1753 (1981).

[8] T. Miller and T.-C. Chiang, Phys. Rev. Lett. **68**, 3339 (1992).

[9] A. Hasegawa, S. Wakoh, and J. Yamashita, J. Phys. Soc. Jpn. **20**, 1865 (1965).

[10] For a review, see J. B. Sokoloff, Phys. Rep. **126**, 189 (1985).

[11] Ivan K. Schuller, M. Grimsditch, F. Chambers, G. Devane, H. Vanderstraeten, D. Neerinck, J.-P. Locquet, and Y. Bruynseraede, Phys. Rev. Lett. **65**, 1235 (1990).

[12] M. Luban, J. H. Luscombe, and B. N. Harmon, Solid State Commun. **51**, 199 (1984); M. Luban, and J. H. Luscombe, Phys. Rev. B **35**, 9045 (1987); M. Luban, J. H. Luscombe, and Sihong Kim, Phys. Rev. Lett. **60**, 2689 (1988).

[13] J. L. Perez-Diaz and M. C. Munoz, Phys. Rev. B **50**, 8824 (1994); J. R. Anderson, D. A. Papaconstantopoulos, L. L. Boyer, and J. E. Schirber, *ibid.* **20**, 3172 (1979).

[14] J. H. Luscombe, R. Aggarwal, M. R. Reed, W. R. Frensley, and M. Luban, Phys. Rev. B **44**, 5873 (1991).

[15] See, for example, J. S. Dugdale, *The Electrical Properties of Metals and Alloys* (Edward Arnold, London, 1977), Chap. 7; G. Lehmann and P. Ziesche, *Electronic Properties of Metals* (Elsevier, Amsterdam, 1990), Chap. 5.

[16] I. Mertig, E. Mrosan, and R. Schopke, J. Phys. F **12**, 1689 (1982).